Pathophysiology 26 (2019) 153–162

Contents lists available at ScienceDirect

Pathophysiology

journal homepage: www.elsevier.com/locate/pathophys

Curcuma longa extracts suppress pathophysiology of experimental hepatic parenchymal cell necrosis

David Olawale Adeyemi*, Paul Olugbemiga Awoniran

Department of Anatomy and Cell Biology, Faculty of Basic Medical Sciences, College of Health Sciences, Obafemi Awolowo University, Ile-Ife, Nigeria

ARTICLE INFO

Article history:
Received 28 May 2018
Received in revised form 13 April 2019
Accepted 14 April 2019

Keywords:
Potassium bromate
Curcuma longa
Liver injury
Massive necrosis
Karyorrhexis
Lipid peroxidation

ABSTRACT

The study sought to investigate the protective potentials of *Curcuma longa* rhizome following potassium bromate-induced liver injury in Wistar rats. Thirty-five male Wistar rats were divided into 7 groups of 5 rats each (n = 5). Control group received normal saline while the other groups received oral administration of 100 mg/kg potassium bromate daily for two weeks to induce hepatic injury. Negative control I rats were sacrificed immediately after induction of hepatic injury, while the test groups were given oral dose of ethanol extract of *Curcuma longa* rhizome (EECLOR) at 100, 200 and 400 mg/kg for two weeks. Positive control group was treated with Silymarin for two weeks, while negative control II group was observed for the two-week period. At the end of the study, serum biochemical parameters of liver function enzymes, malondialdehyde and histopathological changes were investigated. Necrotic hepatocytes were quantified in H&E-stained liver sections using the morphologic criteria of typical necrotic tissue. Hepatocytes that remained intact were identified as those with round euchromatic nuclei with prominent nucleoli. Histological examination and morphological grading of the stained sections showed massive necrosis across the zones. EECLOR improved liver functions evidenced by reduced activity of serum amino transferases. It also reduced lipid peroxidation. In addition, there was significant reduction of hepatocytes showing morphological criteria of necrosis in EECLOR-treated rats across the zones, with appreciable radial sinusoidal arrangement. In conclusion, the protective actions of EECLOR against potassium bromate liver toxicity in rats, appears to be due to its ability to reduce lipid peroxidation.

1. Introduction

The ban on potassium bromate ($KBrO_3$) as a food additive has not prevented it from sneaking into food products [1]. It has been discovered in refined flour products including burger and pizza. In some other products found on supermarket shelves, including toothpastes and mouthwashes, it is added as an antiseptic and astringent [2]. It also forms a major constituent in fumigants for agricultural pest control, flame retardants, reagents for printing, prescription drugs and cosmetics as permanent wave neutralizer [2]. Furthermore, $KBrO_3$ is used in laboratories as an analytical and strong oxidizing reagent in organic and inorganic reactions [3,4]. It is found in water disinfected by ozonation and consequently frequently detected in ozonized water [5]. Being a bio-stable substance, $KBrO_3$ crosses biological membrane easily to cause intracellular toxicity [6] and has been associated with hepatotoxicity, neurotoxicity, nephrotoxicity and carcinogenesis [7]. According to scientists, there is no safe level of exposure to a carcinogen [8] as it is considered to exert its toxicity through the basic mechanism of lipid peroxidation, leading to generation of free radicals [9]. Various researchers have shown that potassium bromate induces necrosis and distorts cellular architecture [10,11] but have left out a specific report on the cytoplasmic and nuclear changes, the zonal extent of these damages as well as the conflict of ideas on the antidote for bromate toxicity.

Curcuma longa rhizome is a plant food comprising of various compounds closely related to human health [4]. It releases its active constituents to water and alcohol [12]. The main components of the rhizomes are volatile oil and a group of coloring agents called curcuminoids which include curcumin, demethoxycurcumin, 5-methoxycurcumin and dihydrocurcumin with curcumin, a polyphenol compound, which is the most important fraction [12].

This investigation evaluates sequential centrilobular, mid-zonal and periportal nuclear as well as cytoplasmic changes in hepatic parenchymal cells of rats, following $KBrO_3$ toxicity. It futher assessed the effects of ethanol extract of *C. longa* rhizome on the histomorphology, morphometry and biochemical parameters of liver tissue of rats with $KBrO_3$-induced alterations.

* Corresponding author.
E-mail address: waledavade@yahoo.com (D.O. Adeyemi).

https://doi.org/10.1016/j.pathophys.2019.04.002
0928-4680/

2. Materials and methods

2.1. Chemicals

Potassium bromate (P28/65/455-1), procured from May and Baker Limited, Dagenham, England. Silymarin tablet (SYFH0048), procured from Micro Labs Limited, India. ALP, AST and ALT assay kits were purchased from RANDOX Laboratories Limited, Ardmore, United Kingdom. Other reagents used were of analytical grade.

2.2. Preparation of *Curcuma longa* rhizome extract

Fresh *C. longa* rhizomes were purchased from a commercial supplier at Sabo market in Ile-Ife (South-West Nigeria, West Africa). The rhizomes were authenticated by a taxonomist at the Department of Botany, Obafemi Awolowo University, Ile-Ife with the voucher number IFE-17538, for reference purpose. Ethanol extract of *Curcuma longa* rhizome (EECLOR) was prepared using standard procedure. The rhizomes were descaled, air dried and pulverized in a milling machine (DIK - 2913). The pulverized rhizomes were extracted three times with 70% ethanol and continuously stirred at room temperature with a magnetic stirrer for 24 h each. The extracts were filtered using Whatmann No. 1 filter paper. The filtrates were concentrated *in vacuo* at 40 °C using a vacuum rotary evaporator (Buchi). The extracts obtained were stored in a desiccator prior to phytochemical evaluation.

2.3. Phytochemical analysis

Comprehensive screening was carried out to check for the presence or absence of secondary metabolites in the extract. Compounds tested for include: alkaloids, flavonoids, tannins, cardiac glycosides, phenols, phytosterols, saponins, terpenoids lactones, anthraquinone, phlobatannin and proteins. All tests were carried out as previously described [13].

2.4. Animal care and management

The thirty-five male Wistar rats (120–150 g) used for this study were bred at the animal holding of the Department of Anatomy and Cell Biology, Obafemi Awolowo University, Ile-Ife and housed in plastic cages under standard laboratory conditions. The rats fed on standard laboratory rat chow (ACE feed, Osogbo, Nigeria,) and had access to water *ad libitum*. Ethical clearance (Clearance no: IPH/OAU/12/813) was obtained from the Health Research and Ethics Committee (HREC) of the Institute of Public Health, Obafemi Awolowo University, Ile-Ife. The rats received humane care according to the criteria stipulated in the Guide for Care and Use of Laboratory Animals, prepared by the National Institute of Health [14].

2.5. Experimental

2.5.1. Experimental design

Thirty-five male Wistar rats (120–150 g) were randomly assigned into 7 groups (n = 5) thus:

Group 1 (*Normal control group*) received normal saline orally for 28 days; **Group 2** (*Br. Only*) received 100 mg/kg $KBrO_3$ daily for 14 days and were sacrificed 24 h after the last dose was administered; **Group 3** (*Br. + 100 mg/kg E*) were pre-treated with 100 mg/kg $KBrO_3$ daily for 14 days and later received 100 mg/kg EECLOR daily for 14 days; **Group 4** (*Br. + 200 mg/kg E.*) first received 100 mg/kg $KBrO_3$ daily for 14 days and were subsequently administered 200 mg/kg EECLOR daily for 14 days**;** **Group 5** (*Br. + 400 mg/kg E.*) were administered 100 mg/kg $KBrO_3$ daily for 14 days and then received 400 mg/kg EECLOR daily for 14 days, **Group 6** (*Br. + Silymarin*) rats also received 100 mg/kg $KBrO_3$ daily for 14 days and were later treated with 2 mg/kg Silymarin 12 hourly for 14 days. Finally, **Group 7** (*Br. + Observation*) rats received 100 mg/kg $KBrO_3$ daily for 14 days and were observed for the subsequent 2 weeks before sacrifice.

2.5.2. Determination of body weight

All the rats were weighed individually with a top loader digital balance every 3 days prior to commencement of the experiment and afterwards to assess any change in body weight over time. Body weight change was expressed as the percentage difference between the final and initial body weights, divided by initial weight.

$$Percentage\ weight\ change = \frac{final\ weight - initial\ weight}{initial\ weight} x\, 100\%$$

2.5.3. Sacrifice and surgical excision of the liver

At the end of the experiment, the rats were sacrificed under diethyl ether anesthesia. A midline abdominal incision was made on each rat and whole liver was excised, carefully trimmed of ligaments, peritoneal covering and weighed on a top loader digital balance. Because liver lobes respond to hepatotoxic agents differently [15], all samples were taken from median lobe (Fig.1) leaving out the left, right and caudate lobes. Relative liver weight was defined as the percentage ratio of liver weight to final body weight.

$$\text{Relative organ weight} = \frac{\text{organ weight}}{\text{final body weight}} \times 100\%$$

2.5.4. Histological procedure

The median lobe of each rat liver was grossed into two pieces and fixed in Neutral Buffered Formalin (NBF) for histological demonstrations. The tissues were kept in the fixative at room temperature till processed. The second pieces were frozen for the estimation of malondialdehyde. Tissues were processed via paraffin wax embedding method [16], 5 μm thick sections were obtained on a rotary microtome (Leica RM 2125 RTS) and stained with hematoxylin and eosin (H & E) for the demonstration of general histoarchitecture and evaluation of necrotic changes.

2.5.5. Photomicrography

The liver sections were examined under a LEICA research microscope (DM750) connected to a digital camera (LEICA ICC50) and permanent photomicrographs were taken. Scale bars were merged on each micrograph taken.

2.5.6. Image analysis

Integrated morphology analysis was undertaken using image J software. Digital bright field images were uploaded unto the image J analysis software. The scale was set using a digital micrometer gauge reading to convert measurements in pixels to microns and this was applied to all images. Cells were counted using the cell counter plug-in available on the image *J* analysis software, after a grid (4000 μm^2) had been applied across the images.

2.5.7. Serum sampling for biochemical assay

At sacrifice, blood samples were collected by cardiac puncture into plain bottles and centrifuged at 3000 rpm for 10 min (after clotting at room temperature) to obtain serum.

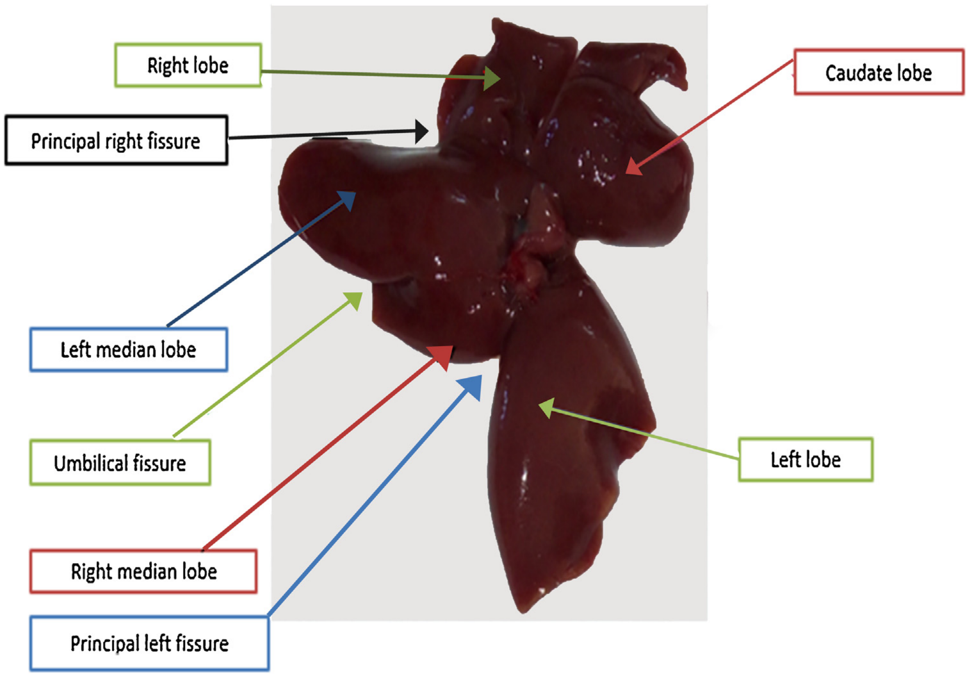

Fig. 1. Photograph of rat liver showing its lobes.

Table 1
Quantification of necrotic change.

Percentages of occurrence	Grades	Grades indication
0	0	None
<20	1+	Mild
20–70	2+	Marked
>70	3+	Severe

2.6. Assessment of hepatotoxicity

2.6.1. Histological scoring

Quantification of cellular death and intact hepatocytes were carried out as follows: the number of necrotic hepatocytes were counted in 10 high power fields (HPF) (400x) of H & E stained sections, taking account of the following morphological criteria: increased eosinophilia, cell swelling and lysis, intracytoplasmic vesiculation, intra-nuclear vacuolation, plasmorhexis, plasmolysis, karyolysis and karyorrhexis around the periportal (zones 1), mid-zonal (zone 2) and centrilobular areas (zone 3) of hepatic plates [17–19]. Further support for these criteria came from the observation that the damaged cells form a confluent area, which is characteristic of oncotic necrosis as against apoptosis [19]. Intact hepatocytes were defined as those with round nuclei with prominent nucleoli [20]. All specimens were examined for these features. The percentage of necrotic changes observed was estimated by evaluating the number of microscopic fields with necrosis, compared to the whole histologic sections. Severity in necrotic changes in each liver was graded following a modification of a previously reported model [21] shown in Table 1.

2.6.2. Assessment of liver function markers

The serum activities of aspartate aminotransferase (AST), alanine aminotransferase (ALT) and alkaline phosphatase (ALP) were measured to assess hepatotoxicity. Activities of AST, ALT and ALP were measured in the serum, using enzyme colorimetric assay kits using standard procedures.

2.6.3. Assessment of hepatic lipid peroxidation

To estimate level of tissue malondialdehyde (MDA), each frozen median lobe was homogenized in 10 mL of sucrose solution using an electric homogenizer. Lipid peroxidation was estimated as described by Ohkawa et al. [22]; 0.5 mL of phosphate buffer (0.1 M, pH 8.0) and 0.5 mL of 24% trichloroacetic acid (TCA) were added to 0.5 mL of samples. The resulting mixture was incubated at room temperature for 10 min and centrifuged at 2000 rpm for 20 min to obtain a supernatant. To every 1 mL of supernatant, 0.25 mL of (0.33%) thiobarbituric acid (TBA) in 20% acetic acid was added, and the resulting mixture was boiled at 95 °C for 1 h. The resulting **pink** coloured product was cooled and the product's absorbance was read at 532 nm (Extinction coefficient of MDA, $\varepsilon 532 = 1.53 \times 105$ M-1 cm-1).

2.7. Statistical analysis

Results were expressed as Mean ± S.E.M. GraphPad Prism5 (Version 5.03, GraphPad Inc.) was used to carry out all statistical analyses. Data were analyzed using one-way analysis of variance (ANOVA), followed by Students Newman-Keuls (SNK) and Dunnett post hoc tests for multiple comparisons. Results were considered significant at $p < 0.05$.

3. Results

3.1. Phytochemical constituents of Curcuma longa

The phytochemical screening of ethanol extracts of *Curcuma longa* rhizomes in this study revealed the following constituents: alkaloids, flavonoids, saponins, phlobatanin, tannins, terpenoids, phytosterols, phenols and anthraquinones (Table 2). Curcuminoids, a polyphenolic compound had been previously isolated from turmeric rhizomes [23,24]. On screening, the curcuminoids complex found in turmeric rhizome include curcumin, demethoxycurcumin and bisdemethoxycurcumin. The chemical structures of

Table 2
Phytochemical screening of ethanol extract of *Curcuma longa* rhizome.

Class of compounds		Ethanol extract
	Mayer's reagent	++
Alkaloids	Wagner's reagent	++
	Drangedorf reagent	++
Cardiac glycosides		–
Flavonoids		+
Saponins		++
Phlobatanin		+
Tannins		+
Terpenoids		+
Phytosterols		+
Phenols		++
Anthraquinones		+
Lactone		–
Protein		–

Note: (–): Absence; (+): Less presence; (++): Moderate presence.

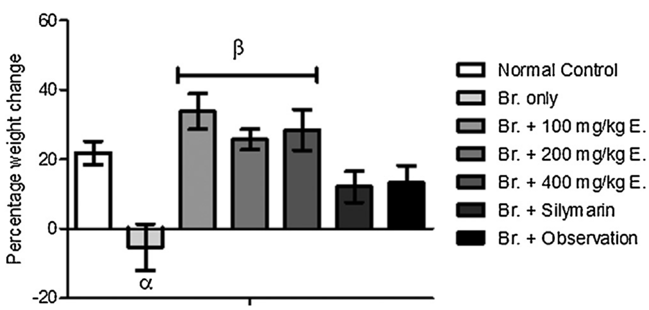

Fig. 2. Effects of EECLOR on percentage weight change (PWC) of Wistar rats exposed to $KBrO_3$ toxicity. Data are mean ± S.E.M. α- significantly different from normal control, β- significantly different from negative control at $p < 0.05$.

these constituents and their percentage composition are shown in Table 3 [23,24].

3.2. Effects of EECLOR on percentage weight change and relative organ weight of rats with $KBrO_3$ - induced hepatic injury

Potassium bromate caused significant weight loss in *Br. + Silymarin*, *Br. Only and Br. + Observation* groups when compared with normal control ($p = 0.01$) (Fig. 2).

However, in a dose-independent manner, the extract significantly restored body weight of rats in the test groups (*Br. + 100 mg/kg E*, *Br. + 200 mg/kg E* and *Br. + 400 mg/kg E*) when compared with *Br. Only* group ($p = 0.0004$); there was no significant difference in the weight gain of test groups and that of the *Br. + Silymarin* group ($p = 0.0647$) (Fig. 2). Consequently, treatments

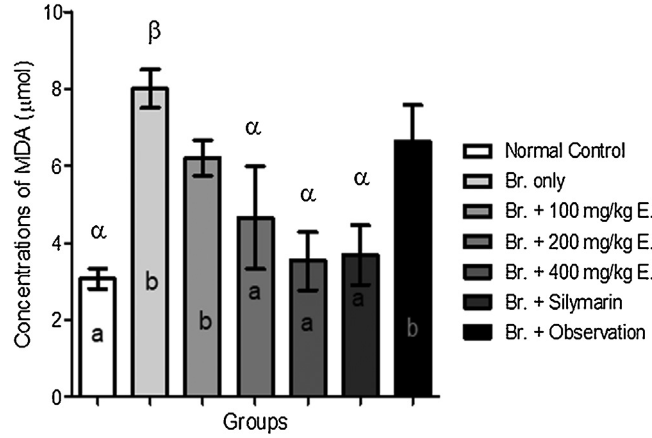

Fig. 3. Effects of EECLOR on liver lipid peroxidation product (MDA). Each bar represents Mean ± SEM. Groups with the same alphabet are not significantly different while those with different alphabets are significantly different (SNK). (α) significantly different from negative control, (β) significantly different from positive (Silymarin-treated) control (Dunnett) at $p < 0.05$. MDA - malondialdehyde.

with potassium bromate and *Curcuma longa* extract had no significant effect on relative liver weight of rats across the groups (Table 4).

3.3. Effects of EECLOR on MDA level of rats with $KBrO_3$-induced hepatic injury

Fig. 3 illustrates the effects of extracts of *Curcuma longa* rhizome on tissue MDA level of rats with potassium bromate-induced hepatic injury. Potassium bromate increased significantly the product of tissue lipid peroxidation in *Br. Only and Br. + Observation* groups when compared with the normal control group ($p = 0.004$). However, the extract at doses 200 and 400 mg/kg reduced significantly, the liver concentration of MDA in *Br. + 200 mg/kg E* and *Br. + 400 mg/kg E* groups when compared with *Br. Only* group ($p = 0.03$). This decrease occurred in a manner similar to the significant reduction observed in Silymarin-treated rats ($p = 0.009$). Rats in *Br. + 200 mg/kg E*, *Br. + 400 mg/kg E* groups and *Br. + Silymarin* showed no significant difference in MDA levels compared with the normal control rats ($p = 0.64$).

3.4. Effects of EECLOR on serum activities of liver function enzymes of Wistar rats with $KBrO_3$-induced hepatic injury

Figs. 4–6 illustrate the effects of *Curcuma longa* rhizome extract on the activities of ALP, AST and ALT respectively, in the serum

Table 3
Chemical structure of curcuminoids isolated from *Curcuma longa* rhizome.

Compound	Chemical structure	% Composition
Curcumin	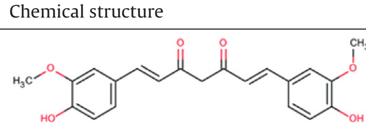	**94**
Demethoxycurcumin	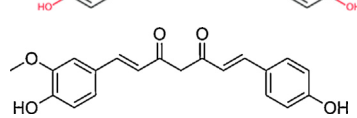	**6**
Bisdemethoxycurcumin	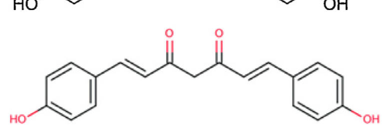	**0.3**

Table 4
Absolute and relative organ weights of male Wistar rats following exposure to $KBrO_3$ and treatment with EECLOR.

Group (n = 5)	Treatment	Absolute weight (g)	Relative weight (%)
Normal control	Normal saline	5.64 ± 0.32	3.52 ± 0.18
Negative control I	100 mg/kg $KBrO_3$	4.96 ± 0.31	3.86 ± 0.43
Test group I	100 mg/kg $KBrO_3$ + 100 mg/kg EECLOR	6.34 ± 0.48	3.60 ± 0.22
Test group II	100 mg/kg $KBrO_3$ + 200 mg/kg EECLOR	5.56 ± 0.37	3.39 ± 0.25
Test group III	100 mg/kg $KBrO_3$ + 400 mg/kg EECLOR	6.8 ± 0.45	4.06 ± 0.12
Positive control	100 mg/kg $KBrO_3$ + 2 mg/kg Silymarine	5 ± 0.62	3.68 ± 0.18
Negative control II	100 mg/kg $KBrO_3$ + 2 weeks observation	6.84 ± 0.33	4.35 ± 0.18
			F = 1.876; p = 0.1203

Values are mean ± SEM of five rats in each group.

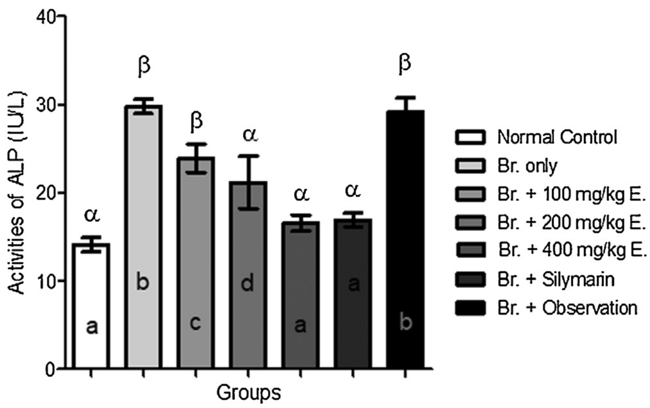

Fig. 4. Effects of EECLOR on serum ALP activity. Each bar represents Mean ± SEM. Groups with the same alphabet are not significantly different while groups with different alphabets are significantly different. (α) significantly different from negative control, (β) significantly different from positive (Silymarin-treated) control (Dunnett) at $p < 0.05$. ALP - Alkaline phosphatase.

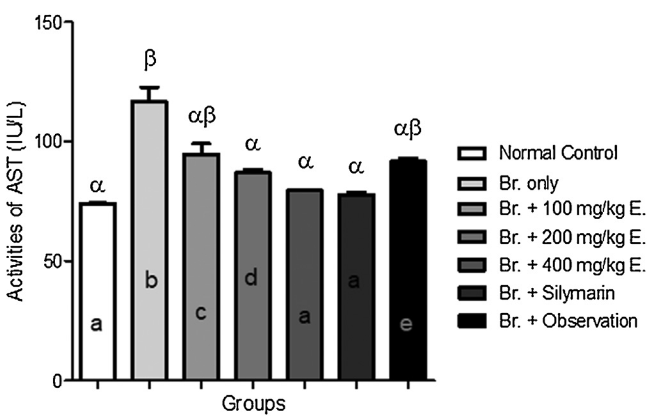

Fig. 5. Effects of EECLOR on serum AST activity. Each bar represents Mean ± SEM. Groups with the same alphabet are not significantly different while groups with different alphabets are significantly different (SNK). (α) significantly different from negative control, (β) significantly different from positive (Silymarin-treated) control (Dunnett) at $p < 0.05$. AST - Aspartate aminotransferase.

of rats with potassium bromate-induced hepatic injury. Results indicated that potassium bromate significantly increased serum activities of ALP, AST and ALT in *Br. Only and Br. + Observation* groups when compared with the normal control group ($p = 0.0001$, $p = 0.0004$, $p < 0.00001$ respectively). However, the extract at every administered dose significantly lowered the serum activities of these enzymes in *Br. + 100 mg/kg E, Br. + 200 mg/kg E* and *Br. + 400 mg/kg E* groups in a dose dependent fashion, when compared with *Br. Only* group ($p = 0.005$, $p < 0.0006$, $p < 0.0001$ respectively). These changes were in a manner similar to the reduction observed in Silymarin-treated positive control rats ($p = 0.0004$, $p = 0.0030$, $p < 0.0001$ respectively). The ALP and ALT activities of

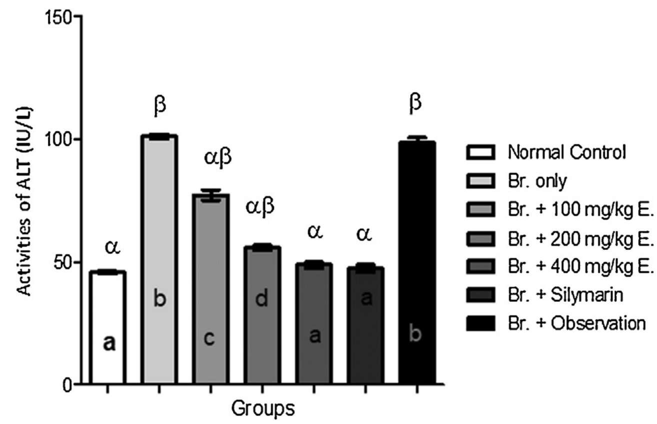

Fig. 6. Effects of EECLOR on serum ALT activity. Each bar represents Mean ± SEM. Groups with the same alphabet are not significantly different while groups with different alphabets are significantly different (SNK). (α) significantly different from negative control, (β) significantly different from positive (Silymarin-treated) control (Dunnett) at $p < 0.05$. ALT - Alanine aminotransferase.

rats in *Br. + 400 mg/kg E* and *Br. + Silymarin* groups were not significantly different from normal control group ($p = 0.11$, $p = 0.27$ respectively).

3.5. Light microscopy report

3.5.1. Histological study

As depicted in Figs. 7 and 8, histopathological examination of H & E stained sections around zones 1, 2 and 3 revealed polyhedral hepatocytes with prominent central vein, eccentrically placed rounded euchromatic nuclei with prominent nucleoli and endothelial cells lining the radially apparent sinusoids in normal control rats. The liver section of rats in *Br. Only and Br. + Observation* groups revealed confluent areas of necrosis with numerous cytoplasmic and nuclear necrotic morphological changes extending from zone 1 through 3. The observed changes include intra nuclear vacuolation, intracytoplasmic vesiculation, karyopyknosis, karyorrhexis and karyolysis, plasmohexis and plasmolysis. These groups also showed distorted architecture with sinusoidal derangement. Rats in *Br. + 100 mg/kg E* group also presented most of these abnormal morphological features in most of the micrographs examined. However, rats in *Br. + 200 mg/kg E* and *Br. + 400 mg/kg E* groups showed predominantly normal architecture with very few abnormal features (Figs. 7 and 8).

3.5.2. Percentage intact and necrotic hepatocytes score

Quantified necrotic hepatocytes across the zones showed 100% intact hepatocytes in the normal control rats across the 10 high-power fields considered. The number of intact hepatocytes decreased significantly in the *Br. Only, Br. + Observation* and *Br. + 100 mg/kg E* groups (40.71%, 39.54%, and 36.92% respectively) when compared with normal control ($p < 0.0001$). However, a dose

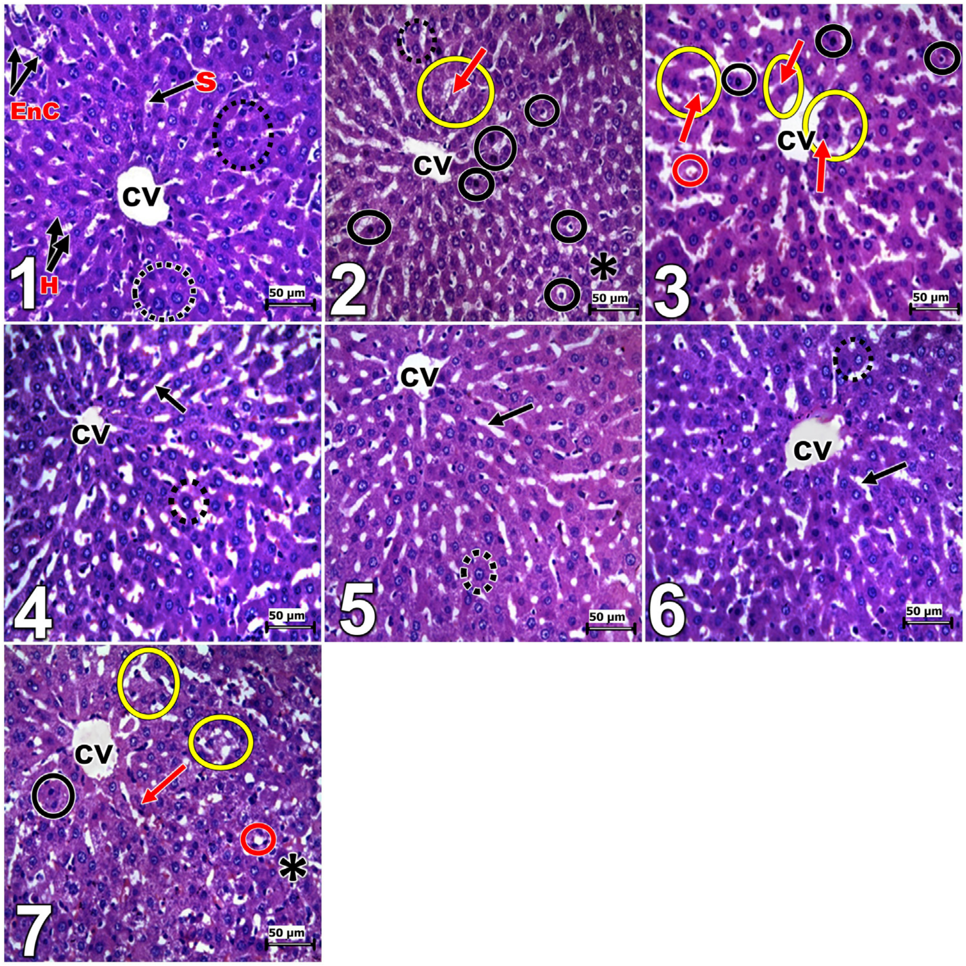

Fig. 7. [1–7] Representative light micrographs of sections of liver subjected to H&E stain at zone 3. Observe in [1] hepatocytes (H) polyhedral in shape with prominent central vein (CV), eccentrically placed rounded euchromatic nuclei with prominent nucleoli (fragmented circle) & endothelial cells (EnC) lining the radially apparent sinusoids (**s**). Confluent areas of necrosis around centrilobular regions with dying cells (yellow circle with red arrows), karyopyknosis or early stage of karyolysis (black circle), vesicular nuclei/intranuclear vacuolation (red circle) were observed in [2,3,7]. Sinusoids in [2,7] are not radially apparent and parenchyma cells are abnormal (right -asterisk). Features of the liver structure in [4–6] are close to control [1] with prominent nucleoli (fragmented circle) and radially apparent sinusoids (black arrows). Scale bar = 50 μm [1]. = normal control [2]; = *Br. Only*; [3–5] = *Br. + 100 mg/kg E, Br. + 200 mg/kg E* and *Br. + 400 mg/kg E* respectively; [6] = *Br. + Silymarin*; [7] = *Br. + observation*. (For interpretation of the references to colour in this figure legend, the reader is referred to the web version of this article).

Table 5
Histological scores of liver damages induced by $KBrO_3$ and the effects of EECLOR and Silymarine treatments.

Zonal necrosis (zones 1, 2 and 3)						
		Grade				
Groups	Treatment	0	1+	2+	3+	Average
Normal control	Normal saline	10 (100)	0 (0)	0 (0)	0 (0)	$0^{a\alpha}$
Negative control I	100 mg/kg $KBrO_3$	0 (0)	0 (0)	9 (90)	1 (10)	$59.29^{b\beta}$
Test group I	100 mg/kg $KBrO_3$ + 100 mg/kg EECLOR	0 (0)	0 (0)	8 (80)	2 (20)	$63.08^{b\beta}$
Test group II	100 mg/kg $KBrO_3$ + 200 mg/kg EECLOR	0 (0)	2 (20)	8 (80)	0 (0)	$31.74^{c\alpha\beta}$
Test group III	100 mg/kg $KBrO_3$ + 400 mg/kg EECLOR	8 (80)	1 (10)	1(10)	0 (0)	$3.858^{a\alpha}$
Positive control	100 mg/kg $KBrO_3$ + 2 mg/kg Silymarine	7 (70)	2 (20)	1 (10)	0 (0)	$5.375^{a\alpha}$
Negative control II	100 mg/kg $KBrO_3$ + 2 weeks observation	0 (0)	0 (0)	7 (70)	3 (30)	$60.46^{b\beta}$

Numbers of high power fields are shown, with percentages enclosed within parenthesis. n = 5. Grade indication: no change (0), mild (1+), marked (2+), severe (3+) (0; 0%, 1+; less than 20%, 2+; 20–70%, 3+; more than 70% of hepatic plate). Groups with the same alphabet are not significantly different while groups with different alphabets are significantly different (SNK). (α) are significantly different from negative control (group 2), (β) are significantly different from silymarine treated group (positive control) [Dunnett] at $p < 0.05$.

dependent significant increase in intact hepatocytes ($p < 0.0001$) was quantified in *Br. + 200 mg/kg E* and *Br. + 400 mg/kg E* groups (68.29% and 96.14% respectively) when compared with the *Br. Only* group. The value at the highest dose was comparable to the 94.63% intact hepatocytes quantified in the positive control group (Fig. 9). Histological scoring of severity of necrosis in the liver sections is as presented in Table 5

4. Discussion

Liver injury and the resulting dysfunction represent life-threatening conditions that require immediate intervention. Healthy plant materials contain naturally occurring, vast assortment of chemical compounds, both organic and inorganic [25]. These chemicals are secondary metabolites that enable plants over-

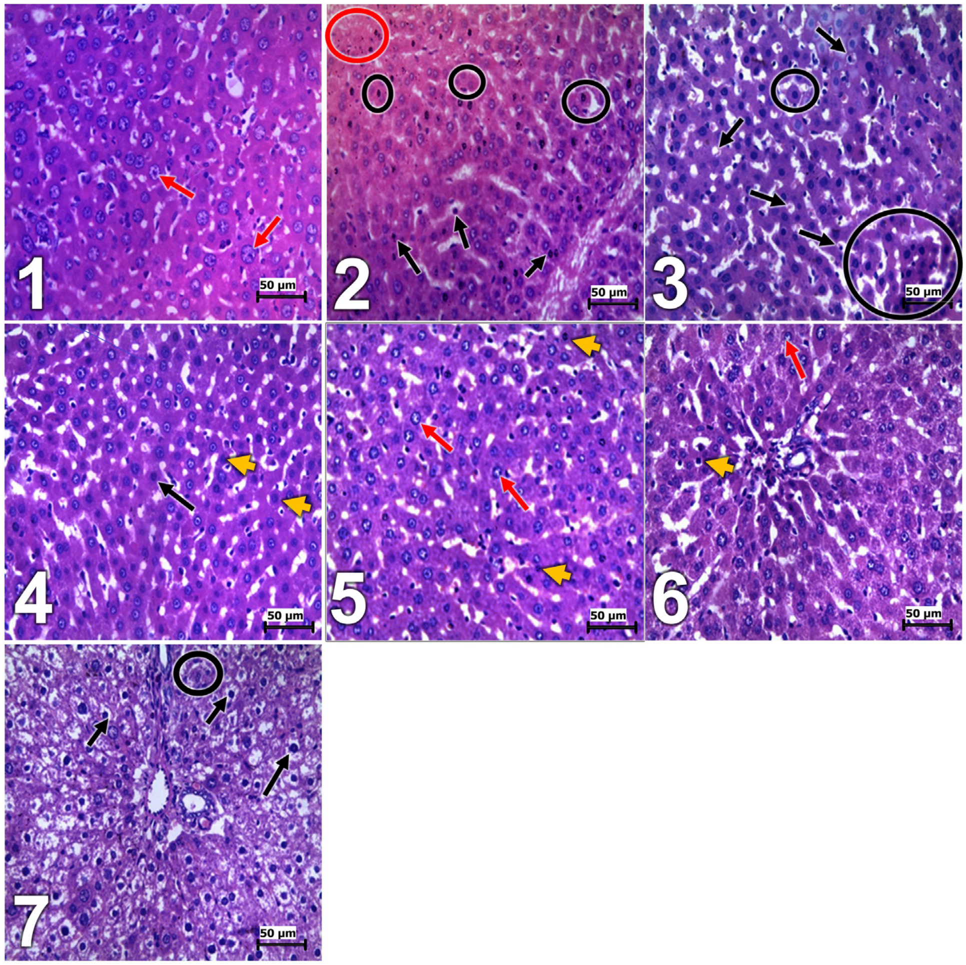

Fig. 8. [1–7]: Representative light micrographs of sections of liver subjected to H&E stain at zone 2 of hepatic acini. Observe in [1] polyhedral hepatocytes having round nuclei with prominent nucleoli (red arrows). In [2,3,7] dying hepatocytes (black circle) with increased eosinophilia, pyknosis (black arrows), karyolysis and karyorrhexis (red circle) were observed. In [4–6] intact hepatocyte nuclei (red arrows) with scanty pyknotic ones (yellow arrow heads) were observed. Scale bar = 50 µm. [1] = normal control [2]; = *Br. Only;* [3–5] = *Br. + 100 mg/kg E, Br. + 200 mg/kg E* and *Br. + 400 mg/kg E* respectively; [6] = *Br. + Silymarin*; [7] = *Br. + observation*. (For interpretation of the references to colour in this figure legend, the reader is referred to the web version of this article).

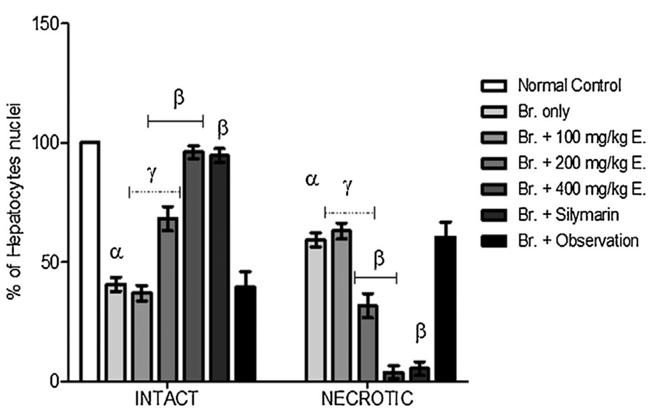

Fig. 9. Hepatocytes nuclei count of H&E stained sections of the liver (zones 1, 2 and 3 of hepatic acini). Values are expressed as mean ± SEM. α – significantly different from normal control, β - significantly different from negative control, γ - significantly different from Silymarin-treated group at $P < 0.05$.

come threats integral to their environment by contributing to the innate immunity as phytoprotectants [26]. They are beneficial to humans for their therapeutic abilities [4]. In this study, *Curcuma longa* rhizome has been screened for its phytochemicals, including alkaloids, flavonoids, saponins, phlobatanin, tannins, terpenoids, phytosterols, phenols and anthraquinones. These secondary metabolites are reported to have many biological and therapeutic properties. They are associated with treatment of cellular injuries resulting from free radicals, chronic diseases such as cardiovascular disease, liver injury, cancers, as well as other medical conditions [25,27].

In this study, rats in *Br. Only* group showed significant weight loss when compared with normal control rats. Potassium bromate in this case can be said to have body weight reduction capabilities. Abdel et al. [28] also reported weight loss in $KBrO_3$ - administered rats. However, the weight gain observed in EECLOR-treated rats point to the weight enhancing ability of the extract. This result is in line with the report of El-Banhawey et al. [29] which reported that *C. longa* enhanced body weight in mice.

It was observed in this study that potassium bromate exerts no significant difference on the relative liver weight of experimental rats when compared with control group rats, a pointer to the fact that potassium bromate toxicity is not associated with hepatomegaly or whole organ shrinkage. This result is consistent with the reports of Dimkpa et al. [30] and Farombi et al. [31] in which they reported that potassium bromate treatment had no effect on liver/body weight ratio in rats.

Furthermore, there was an increase in tissue level of malondialdehyde, a major reactive aldehyde resulting from the peroxidation of biological membranes showed in the *Br. + 100 mg/kg*

E (administered with the least dose of EECLOR), *Br. Only* and *Br.+ Observation* groups. The increase is indicative of passive interaction of reactive oxygen species with hepatic parenchymal cell lipids, a cellular macromolecule [32]. The ROS may have been generated from reactive metabolites formed from the metabolism of potassium bromate [7]. Lipid peroxidation has been shown to arise in numerous model systems following exposure to potassium bromate, and is believed to be the key mechanism of toxicity [7,33,34], which agrees with the results of this study. The dose-dependent reduction in MDA levels found in *Br. + 200 mg/kg E*, *Br. + 400 mg/kg E* and *Br. + Silymarin* groups, could be related to the presence of flavonoids, terpinoids and other phenols in EECLOR. Some studies reported that these compounds display a wide range of biological activities and hence have pharmacological effects [35]. Flavonoids and other phenols, in particular, have been reported to react with free radicals to ameliorate the degradation induced by their intense reactivity [26,36]. The mechanism responsible for the activity of flavonoids could be associated with biological membrane stabilization induced by preventing deterioration of polyunsaturated lipids.

A spike in serum amino transferases in *Br. Only*, *Br.+ Observation* and *Br. + 100 mg/kg E* groups was also observed in this study. The level of these metabolic enzymes, which are generally low in the serum is known to increase with the death of hepatocytes [37]. This is suggestive of the fact that there was leakage of these intracellular enzymes into the serum as a result of cell membrane destabilization from hepatocellular necrosis. This corroborates the findings from a number of laboratory studies that also reported an increase in serum amino transferases level, after weeks of potassium bromate administration [30,31,34,38]. Conversely, the significant reduction in serum activity of these enzymes, due to increased concentration of EECLOR, may be related to the inhibition of free radical formation and antioxidative effects of phenolic compounds present in the extract. It is well known that natural antioxidants come mainly from plants in the form of phenolic compounds such as flavonoids, phenolic acids etc. [27,39]. Many reports suggest that plants rich in phenolic content exhibit good antioxidant activity, that is; there is a direct connection between total phenol content and antioxidant activity [40,41].

Also in this study, we observed an increase in the level of serum alkaline phosphatase (ALP). ALPs are found in the hepatocytes and their activities in the serum are usually elevated in cholestasis [42]. A definition of cellular death may be based upon the loss of the general functions of c̈ellular homeostasis;̈ a cell is dead when it is no longer capable of preserving, in a normal environment, the specific composition of its inner milieu [43–45]. In conditions affecting the liver, damaged liver cells release increased amount of ALP into the blood, an indication of the inability of hepatocytes to preserve, in a normal environment, the specific composition of its inner milieu [46]. Taking account of previous similar findings in male Wistar rats [31], it is strongly suggested that potassium bromate impair normal bile flow possibly by exerting oxidative stress and genotoxic effects through the mechanisms of lysosomal damage, an event preceding the oxidative DNA damage. It is shown in this study that turmeric ethanol extract, in a dose-dependent manner, improved the absorbance capacity of oxygen radical in liver tissue; as serum ALP level was found to be low in groups treated with middle and high dose extracts in a fashion similar to the Silymarin-treated rats. This supports previous studies on the hepatoprotective capacity of saponin (a major bioactive compound found in *Curcuma longa* rhizome) against oxidative stress, through the down-regulation of ROS, attenuating protein, and lipid oxidation of hepatocytes [47].

In this study, nuclear and cytoplasmic cell death in rats treated with potassium bromate cuts across the three zones of hepatic acini. According to the hepatic acini conceptualization of the organization of hepatic parenchyma, the parenchymal cells farthest away from the vascular backbone of the acinus have greatest sensitivity to damage from reactive and toxic metabolites, while those nearest to it are least vulnerable [20,48]. The extension across the zones point to the high rate of toxicity induced by this agent, which extended to the areas least expected to be sensitive to toxins. According to a previous report by Lautt [49], the zonality of toxic substances appear to be related to the mechanism of injury and the zonal concentration of the enzyme system responsible for the conversion of the agents to toxic metabolites. In line with this report, we suggest that the massive necrosis observed in this study could be attributed to the dispersed concentration of the enzyme system responsible for the conversion of potassium bromate into its hepatotoxic metabolites across the three zones. The morphological microscopic changes observed are in accordance with the reports of Oyewo et al. [11], Dimkpa et al. [30] and Bayomy et al. [34] in which they demonstrated significant degrees of cell necrosis and cytoplasmic vacuolation in the liver of potassium bromate treated rats. However, karyorrhexis, the predominant nuclear damage observed in this study was not reported in their studies. This may be due to the differences in the mode of oral administration of potassium bromate employed in these studies, as the amount of potassium bromate consumed by these animals in their drinking water may not have been ascertained. The dose dependent reduction in the frequency of nuclear and cytoplasmic necrotic changes observed in rats treated with middle and high dose of EECLOR may be as a result of the hepatoprotective effect of the major constituents of this extract. The tannins present in the extract could alter the progression of cellular damage. In addition, they may also supplement endogenous antioxidants, preventing further oxidative damage. Tannins have been reported to be high-molecular compounds exhibiting usually strong antiradical and antioxidant activities [40,50].

Furthermore, in this study, we observed disrupted sinusoidal radiation in potassium bromate-treated rats, while normal radiating sinusoids were observed in extract treated groups. The hepatic sinusoids correspond to the capillary bed of the liver and represent the segment of hepatic microcirculation in which supply of nutrients, removal of metabolic products and clearance of toxins and foreign bodies from the blood streams take place [21,51,52]. Main sinusoids run straight between the liver cell cords over a length of approximately 250 μm and communicate with each other through shorter interconnecting sinusoids, running across the liver cell cords [52]. These characteristic features of normal sinusoids were seen in the normal control as well as *Br. + Silymarin*, *Br. + 200 mg/kg E and Br. + 400 mg/kg E* groups. This may be responsible for the parenchymal cells found intact in them, as the arrangement may be efficient for the exchange between the blood and the hepatocytes. Paucity of delineable central vein and disorganized sinusoids observed in the *Br. + 100 mg/kg E*, *Br. Only* and *Br.+ Observation* groups, may be a pointer to impairment of hepatic microcirculation which guarantees the supply of parenchymal tissues with oxygen and nutrient. This mal-organization of hepatic parenchyma and microvascular system may be inefficient for the exchange between the blood and the hepatocytes [53]. It may also denote selective damage of sinusoidal endothelial cells demonstrating a formation of large intracellular gaps and a reduction of the diameter of the remaining endothelial fenestrations [54,55]. Oxidative stress and inflammatory reactions may promote hepatic microcirculatory dysfunction, which is known to be a determinant for subsequent hepatic injury [56]. The presence of flavonoids in the extracts could explain the normal radiating sinusoids observed in *Br. + 200 mg/kg E and Br. + 400 mg/kg E* groups. The main property of flavonoids is venoactivity- the ability to decrease capillary permeability and fragility [50]. It could therefore be inferred that flavonoid constituent of the extract may have restored normal hepatic microcirculation, efficient enough for the exchange between blood and hepatocytes in these groups.

5. Conclusion

Data from this study have shown that potassium bromate induced massive necrosis which span across multiple hepatic zones and karyorrhexis was the predominant feature observed. This study also demonstrated the hepatoprotective activity of ethanol extracts of *Curcuma longa* rhizome in attenuating massive hepatic parenchymal cell necrosis, following potassium bromate-induced liver injury in Wistar rats. This study concluded that the hepato-protective action of *Curcuma longa* could be attributed to its high antioxidant activity against reactive oxygen species and its ability to reduce lipid peroxidation

References

[1] J.A.O. Oyekunle, A.S. Adekunle, A.O. Ogunfowokan, G.O. Olutona, O.B. Omolere, Bromate and trace metal levels in bread loaves from outlets within Ile-Ife Metropolis, Southwestern Nigeria, Toxicol. Rep. 1 (2014) 224–230.
[2] A. Starek, B. Starek-Świechowicz, Toxicological properties of potassium bromate, J. Pharmacol. Rep. 1 (3) (2016) 122.
[3] T. Umemura, A. Takagi, K. Sai, R. Hasegawa, Y. Kurokawa, Oxidative DNA damage and cell Proliferation in kidneys of male and female rats during 13 weeks' exposure to potassium bromate ($KBrO_3$), Arch. Toxicol. 72 (5) (1998) 264–269.
[4] G. Yong-Song, H. Qing, Plants consumption and liver health, Evid. Based Complement. Altern. Med. 1 (2015) 20.
[5] H. Ueno, K. Oishi, Y. Sayato, K. Nakamuno, Oxidative cell damage in Kat-Sod assay of oxyhalides as inorganic disinfection byproducts and their occurrence by ozonation, Arch. Environ. Contam. Toxicol. 38 (2000) 1–6.
[6] M. Noguchi, K. Nomata, J. Watanabe, H. Kanetake, Y. Saito, Changes in the gap junctional intercellular communication in renal tubular epithelial cells in vitro treated with renal carcinogens, Cancer Lett. 122 (1998) 77–84.
[7] A.B. DeAngelo, M.H. George, S.R. Kilburn, T.M. Moore, D.C. Wolf, Carcinogenicity of potassium bromate administered in the drinking water to male $B6C3F_1$ mice and F344/N rats, Toxicol. Pathol. 26 (1998) 587–594.
[8] K.S. Crump, Use of threshold and mode of action in risk assessment, Crit. Rev. Toxicol. 41 (8) (2011) 637–650.
[9] Y. Kurokawa, Y. Matsushima, N. Takamura, T. Imazawa, Y. Hayashi, Relationship between the duration of treatment and the incidence of renal cell tumors in male F344 rats administered potassium bromate, Jpn. J. Cancer Res. (Gann) 78 (1987) 358–364.
[10] M.M. Elmahdy, M.H.G. Moussa, S.H. Abd-Elgaied, A.A. Alwazaan, Pathological and Immunohistochemical study of potassium bromated on the liver of rat, Vet. Med. J. Giza 2 (61) (2015) 73–82.
[11] O.O. Oyewo, F.M. Onyije, P.O. Awoniran, Hepatotoxic effect of potassium bromate on the liver of Wistar rats, J. Morphol. Sci. 30 (2013) 107–114.
[12] S.J. Hewlings, D.S. Kalman, Curcumin: a review of its' effects on human health, Foods 6 (10) (2017) 92.
[13] D.O. Adeyemi, V.O. Ukwenya, E.M. Obuotor, O.S. Adewole, Anti-hepatotoxic activities of *Hibiscus sabdariffa* L. in animal model of streptozotocin diabetes-induced liver damage, BMC Complement. Altern. Med. 14 (2014) 277.
[14] National Research Council (NRC) Institute of Laboratory Animal Research (ILAR) Guide for the Care and Use of Laboratory Animals, 8th edition, National Academy Press, Washington DC, 2011.
[15] T.A. Lawson, A.W. Pound, The different susceptibility of rat liver Lobes to Carbon tetrachloride and Dimethylnitrosamine, Br. J. Exp. Path. 55 (6) (1974) 583–588.
[16] R.A. Drury, E.A. Wallington, Carleton's Histological Technique, fifth edition, Oxford University Press, London, England, 1980.
[17] A.L. Edinger, C.B. Thompson, Death by design: apoptosis, necrosis and autophagy, Curr. Opin. Cell Biol. 16 (6) (2004) 663–669.
[18] J.S. Kim, L. He, J.J. Lemasters, Mitochondrial permeability transition: a common pathway to necrosis and apoptosis, Biochem. Biophys. Res. Commun. 304 (3) (2003) 463–470.
[19] J.S. Gujral, T.R. Knight, A. Farhood, M.L. Bajt, H. Jaeschke, Mode of cell death after acetaminophen overdose in mice: apoptosis or oncotic necrosis? Toxicol. Sci. 67 (2) (2002) 322–328.
[20] B. Young, J.S. Lowe, A. Stevens, J.W. Heath, Wheater's Functional Histology, a Text and Colour Atlas, fifth edition, Churchill Livingstone, London, United Kingdom, 2006.
[21] A. Naiki-Ito, M. Asamoto, T. Naiki, K. Ogawa, S. Takahashi, S. Sato, T. Shirai, Gap junction dysfunction reduces acetaminophen hepatotoxicity with impact on apoptotic signaling and connexin 43 protein induction in rat, Toxicol. Pathol. 38 (2) (2010) 280–286.
[22] H. Ohkawa, N. Ohishi, K. Yagi, Assay for lipid peroxides in animal tissues by thiobarbituric acid reaction, Anal. Biochem. 95 (2) (1979) 351–358.
[23] A. Bagchi, Extraction of curcumin, IOSR J. Environ. Sci. Toxicol. Food Technol. 1 (3) (2012) 1–16.
[24] H.A. Pawar, A.J. Gavasane, P.D. Choudhary, A novel and simple approach for extraction and isolation of curcuminoids from turmeric rhizomes, Nat. Prod. Chem. Res. 6 (2018) 300.
[25] M. Polovka, V. Brezova, A. Stasko, Antioxidant properties of tea investigated by EPR spectroscopy, Biophys. Chem. 106 (1) (2003) 39–56.
[26] A. Wadood, M. Ghufran, J.S. Babar, M. Naeem, A. Khan, R. Ghaffar, Asnad, Phytochemical analysis of medicinal plants occurring in local area of Mardan, Biochem. Anal. Biochem. 2 (4) (2013).
[27] Ø.M. Anderson, R.K. Markham, Flavonoids: Chemistry, Biochemistry, and Applications, CRC Press, Taylor & Francis Group, Boka Raton, London, 2006.
[28] E.H. Abdel Gadir, W.S. Abdel Gadir, S.E.I. Adam, Toxicologic interaction of potassium bromate and *Allium cepa*, *Allium sativum* or sodium selenite in Wistar rats, J. Pharmacol. Toxicol. 2 (2007) 496–501.
[29] M.A. El-Banhawey, M.A. Ashry, A.K. El-Ansary, S.A. Aly, Effect of *Curcuma longa* or parziquantel on *Schistosoma mansoni* infected mice liver histological and histochemical study, Indian J. Exp. Biol. 45 (10) (2007) 877–889.
[30] U. Dimpka, U.U. Ukoha, E.A. Anyabolu, R.C. Uchefuna, L.C. Anikeh, O.J. Oji, E.E. Besong, O.A. Emenjo, Hepatotoxic effects of potassium bromate on adult Wistar rats, J. Biol. Agric. Healthc. 3 (7) (2013) 111–115.
[31] E.O. Farombi, M.C. Alabi, T.O. Alkuru, Kolaviron modulates cellular redox status and impairment of membrane protein activities induced by potassium bromate ($KBrO_3$) in rats, Pharmacol. Res. 45 (2002) 63–68.
[32] P. Daroui, S.D. Desai, T. Li, A.A. Liu, L.F. Liu, Hydrogen peroxide induces topoisomerase I mediated DNA damage and cell death, J. Biol. Chem. 279 (2004) 14587–14594.
[33] G.H. El-Sokkary, Melatonin protects against oxidative stress induced by the kidney carcinogen KBrO3, Neuro Endocrinol. Lett. 21 (2000) 461–468.
[34] N.A. Bayomy, G.M. Soliman, E.Z. Abdelaziz, Effect of potassium bromate on the liver of adult male albino rat and a possible protective role of vitamin C: histological, immunohistochemical, and biochemical study, Anat. Rec. 299 (9) (2016) 1256–1269.
[35] A. Bink, K. Pellens, B.P.A. Cammue, K. Thevissen, Anti-biofilm strategies: how to eradicate Candida biofilms? Open Mycol. J. 5 (2011) 29–38.
[36] B. de las Heras, B. Rodríguez, L. Boscá, A.M. Villar, Terpenoids: sources, structure elucidation and therapeutic potential in inflammation, Curr. Top. Med. Chem. 3 (2003) 171–185.
[37] R. Omer, A.I. Abuelgasim, B. Elmahdi, Effect of potassium bromate on liver and blood constituents of Wistar albino rats, Am. J. Food Technol. 3 (2008) 310–314.
[38] I.N. Happy Ikhajiangbe, D.N. Ezejindu, A.J. Akingboye, Hepatoprotective effects of *Portulaca oleracea* on liver enzymes of potassium bromate induced hepatotoxicity in adult Wistar rats, Int. Inv. J. Med. Med. Sci. 1 (3) (2014) 26–31.
[39] P.Y. Kwo, S.M. Cohen, J.K. Lim, ACG clinical guideline: evaluation of abnormal liver chemistries, Am. J. Gastroenterol. 112 (2017) 18–35.
[40] E.A.A. Elaziz, Z.S. Ibrahim, A.M. Elkattawy, Protective effect of Curcuma longa against CCl_4induced oxidative stress and cellular degeneration in rats, Glob. Vet. 5 (2010) 272–281.
[41] S.S. Ali, N. Kasoju, A. Luthra, A. Singh, H. Sharanabasava, A. Sahu, U. Bora, Indian medicinal herbs as sources of antioxidants, Food Res. Int. 41 (2008) 1–15.
[42] B.R. Thapa, A. Walia, Liver function tests and their interpretation, Indian J. Pediatr. 74 (7) (2007) 663–671.
[43] G. Majno, L.A. Gattuta, T.E. Thompson, Cellular death and necrosis: chemical, physical and morphologic changes in rat liver, Virchows Arch. Pathol. Anat. Physiol. Klin. Med. 333 (1960) 421–465.
[44] B.E. Trump, I.K. Berezesky, S.H. Chang, P.C. Phelps, The pathways of cell death: oncosis, apoptosis, and necrosis, Toxicol. Pathol. 25 (1997) 82–88.
[45] A.C. Giese, Cell Physiology, fourth edition, W.B. Saunders Company, Philadelphia, USA, 1957.
[46] B.F. Trump, I.K. Berezesky, Cellular and molecular pathobiology of reversible and irreversible injury, in: C.A. Tyson, J.M. Frazier (Eds.), Methods in Toxicology, vol. 1b, Vitro Toxicity Indicators. Academic Press, New York, 1994, pp. 1–22.
[47] L. Qu, H. Xin, G. Zheng, Y. Su, C. Ling, Hepatoprotective activity of the total saponins from *Actinidia valvata* Dunn root against carbon tetrachloride-induced liver damage in mice, Evid. Based Complement. Altern. Med. 2012 (2012) 1–13.
[48] K. Miyai, in: R.G. Meeks, S.D. Harrison, R.J. Bull (Eds.), Structural Organization of the Liver, Hepatoxicity, CRC Press, Boca Raton, FL, 1999, pp. 93–138.
[49] W.W. Lautt, Hepatic circulation: physiology and pathophysiology, in: D.N. Granger, J.P. Granger (Eds.), Colloquium Series on Integrated Systems Physiology: from Molecule to Function to Disease, Morgan & Claypool Life Sciences, San Rafael, California, USA, 2009.
[50] C. Girish, B.C. Koner, S. Jayanthi, K.R. Rao, B. Rajesh, S.C. Pradhan, Hepatoprotective activity of picroliv, curcumin and ellagic acid compared to Silymarin on paracetamol induced liver toxicity in mice, Fundam. Clin. Pharmacol. 23 (6) (2009) 735–745.
[51] L.C. Junqueira, J. Carneiro, Basic Histology Text and Atlas, Eleventh Edition, McGraw-Hill, USA, 2005.

[52] B. Vollmar, M.D. Menger, The hepatic microcirculation: mechanistic contributions and therapeutic targets in liver injury and repair, Physiol. Rev. 89 (2009) 1269–1339.
[53] D.H. Cormac, Essential Histology, second edition, J.B. Lippincolt, Philadelphia USA, 1999.
[54] K.K. Sorensen, J. Simon-Santamaria, R.S. McCuskey, B. Smedsrød, Liver sinusoidal endothelial cells, Compr. Physiol. 5 (4) (2015) 1751–1774.
[55] V.C. Cogger, M. Muller, R. Fraser, A.J. McLean, J. Khan, D.G. Le Couteur, The effects of oxidative stress on the liver sieve, J. Hepatol. 41 (2004) 370–376.
[56] N.V. Sonin, J.C. Garcia-Pagan, K. Nakanishi, J.X. Zhang, M.G. Clemens, Patterns of vasoregulatory gene expression in the liver response to ischemia/reperfusion and endotoxemia, Shock 11 (3) (1999) 175–179.